

Electronic Supplementary Information

How intermolecular interactions influence electronic absorption spectra: insights from the molecular packing of uracil in condensed phases

Fangjia Fu, Kang Liao, Jing Ma, Zheng Cheng, Dong Zheng, Liuzhou Gao, Chungen Liu*, Shuhua Li,
and Wei Li*

^aSchool of Chemistry and Chemical Engineering, Key Laboratory of Mesoscopic Chemistry of Ministry
of Education, Institute of Theoretical and Computational Chemistry, Nanjing University, Nanjing,
210023, P. R. China.

Contents

1. Time evolution of the RMSD for uracil in aqueous solution.....	S3
2. Optimized structural parameters of uracil crystal.....	S4
3. The GEBF-QM/MM excitation energies of configurations.....	S5
4. The GEBF-QM/MM average excitation energies of configurations.....	S6
5. Time evolution of the average hydrogen bond (HB) numbers between the uracil and water molecules.....	S7
6. The distributions of solvatochromic shifts for uracil in aqueous solution.....	S8
7. Computational results of dimer, trimer, and tetramer in amorphous uracil.....	S9
8. Comparisons of the experimental and calculated absorption spectra of amorphous uracil.....	S10
9. The reduced density gradient (RDG) analysis of an amorphous pentamer cluster.....	S11
10. T-aggregation packing for amorphous uracil molecules.....	S12
11. Binding energies of all trimers in crystal.....	S13
12. Binding energies of all tetramers in crystal.....	S14
13. The RDG analysis of a tetramer cluster in crystal.....	S15
14. The absorption spectra using virous TDDFT functionals in crystal.....	S16
15. Frontier molecular orbitals of dimer and trimer clusters in crystal.....	S17
16. The electrostatic potentials with charges of uracil in three condensed phases.....	S19
17. The uracil crystal coordinate file optimized by using PBC-GEBF approach.....	S20
18. References.....	S21

1. Time evolution of the RMSD for uracil in aqueous solution

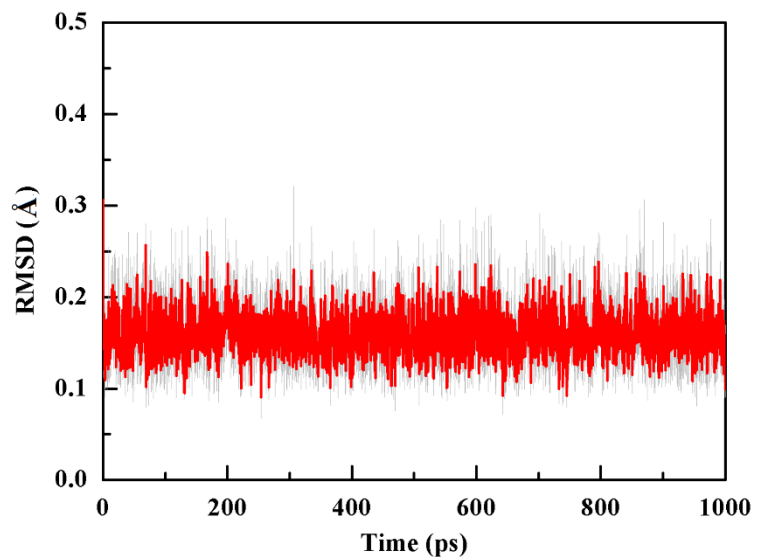


Fig S1. Time evolution of the RMSD for the uracil in aqueous solution.

2. Optimized structural parameters of uracil crystal

Table S1. Comparisons of optimized lattice parameters and experimental parameters of crystal uracil calculated at the PBC-GEBF- ω B97X-D/6-311++G(d, p) level.^{1,2}

Method	a (Å)	b (Å)	c (Å)	α (deg)	β (deg)	γ (deg)	Volume (Å ³)
X-ray	11.938	12.376	3.655	90.0	120.9	90.0	540.0
PBC-GEBF	11.895	12.336	3.569	89.9	121.6	89.8	523.7

3. The GEBF-QM/MM excitation energies of configurations

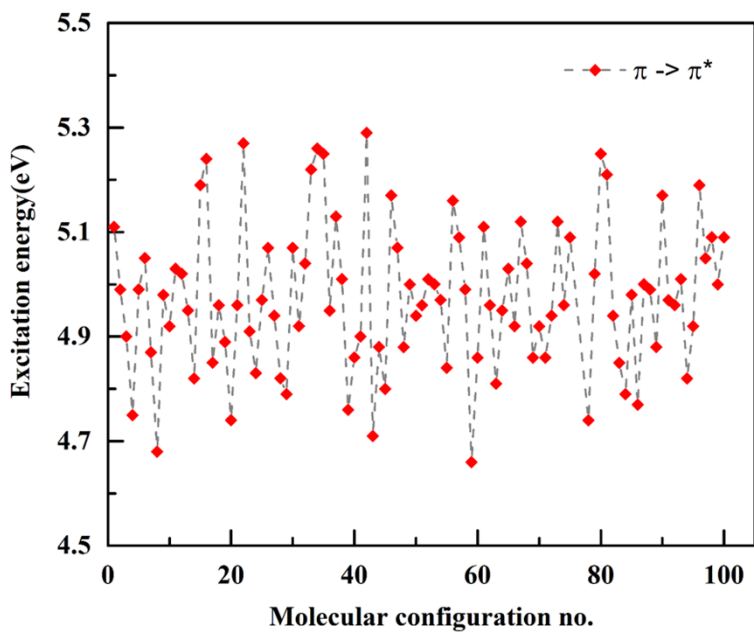


Fig S2. Fluctuations in the excitations energies of uracil in aqueous solution calculated at the GEBF-TD- ω B97X-D/MM level with the 6-311++G(d, p) basis set.

4. The GEBF-QM/MM average excitation energies of configurations

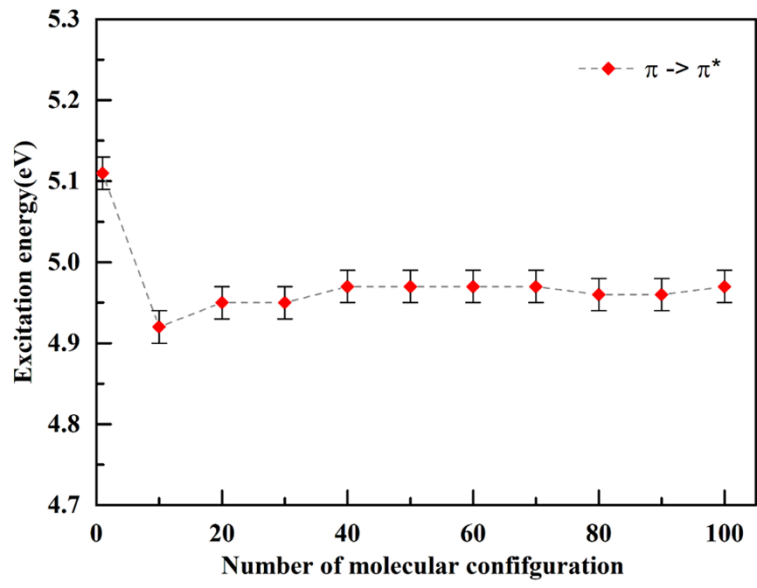


Fig S3. The convergence of average excitation energy as a function of the included number of configurations at the GEBF-TD- ω B97X-D/6-311++G(d, p) level.

5. Time evolution of the average hydrogen bond (HB) numbers between the uracil and water molecules

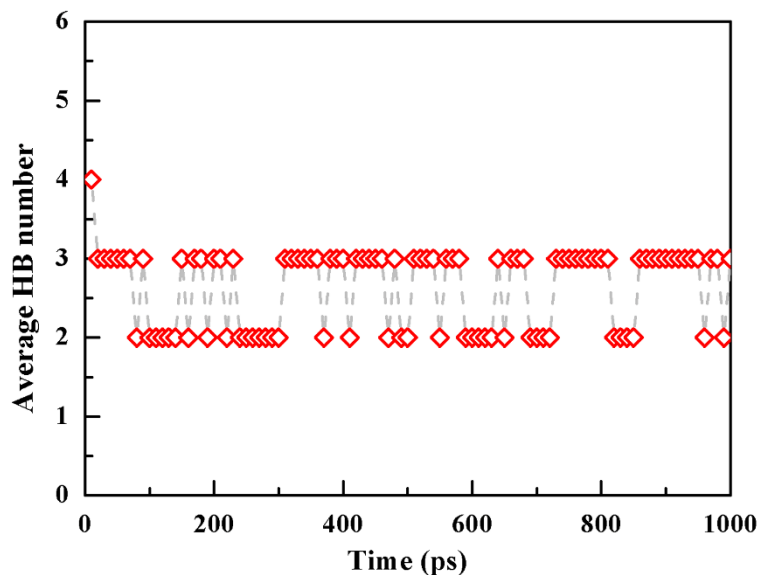


Fig S4. Time evolution of average HB numbers for the uracil and its neighboring water molecules. Each average HB number comes from 100 configurations within 10 ps. Here a HB ($\text{H}-\text{X}\cdots\text{Y}$) is assigned if the $\text{X}\cdots\text{Y}$ length is between 1.5 and 2.2 Å, and the $\text{H}-\text{X}\cdots\text{Y}$ angle is large than 145° .

6. The distributions of solvatochromic shifts for uracil in aqueous solution

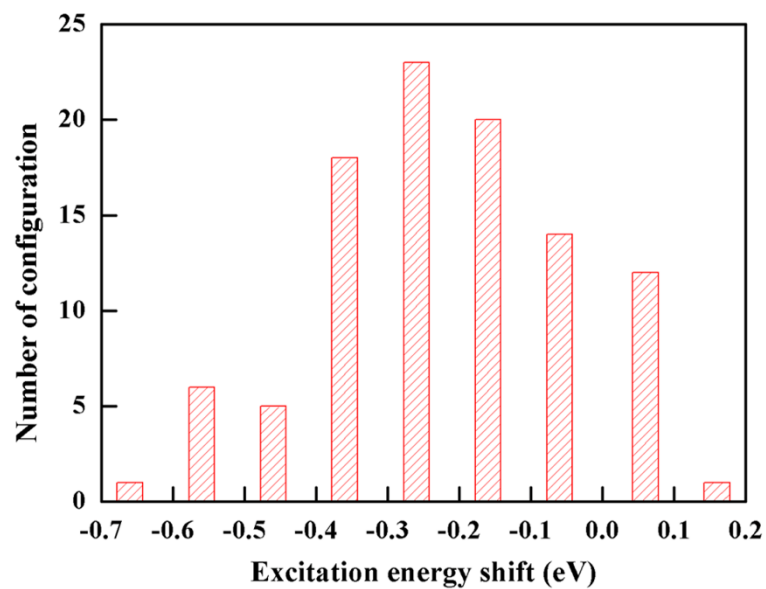


Fig S5. Distributions of the lowest $\pi-\pi^*$ solvatochromic shifts of uracil in aqueous solution calculated at the GEBF-TD- ω B97X-D/6-311++G(d, p) level.

7. Computational results of dimer, trimer, and tetramer in amorphous uracil

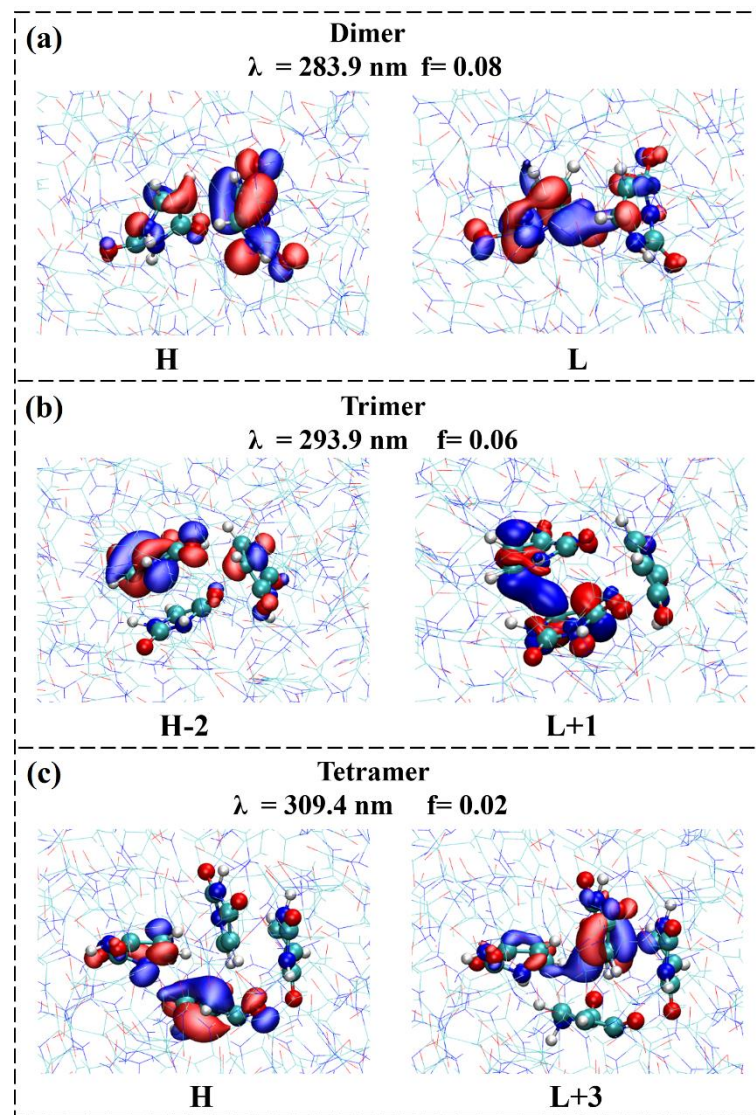


Fig S6. The calculated maximum absorption wavelengths (λ) and oscillator strengths (f) along with the frontier molecular orbitals (H: HOMO, L: LUMO) of dimer, trimer, and tetramer embedded in 10 Å background point charges: (a) dimer, (b) trimer, and (c) tetramer. The structure of the entire system is taken out from the amorphous uracil and just partly MM region are shown in schematic diagram for clarity.

8. Comparisons of the experimental and calculated absorption spectra of amorphous uracil

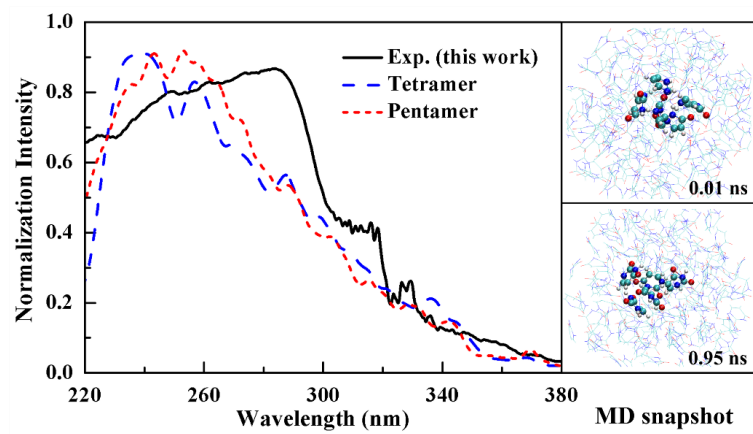


Fig S7. The experimental and calculated (with tetramers and pentamers embedded in background charges) absorption spectra of amorphous uracil. The solid line (in black), dashed line (in blue), and short dashed line (in red) represent the absorption spectra of experiment, tetramer, and pentamer, respectively. Two MD snapshots of amorphous uracil are in right.

9. The reduced density gradient (RDG) analysis of an amorphous pentamer cluster

The RDG can be defined as follows:^{3,4}

$$s(\rho) = \frac{1}{2} (3\pi^2)^{1/3} \frac{|\nabla\rho|}{\rho^{4/3}}$$

where ρ is electron density, and the RDG can be plotted as the function of sign ($\lambda_2\rho$) as shown in Fig S8(b). The λ_2 is the second eigenvalue of Hessian matrix, and “sign” is symbolic function. The RDG function can be employed to distinguish the types of weak interactions.

We employed the Multiwfn program⁵ to analyze the RDG of an amorphous pentamer cluster for non-covalent interactions. For the RDG isosurface figure in Fig S8(a), the blue, green, and red colors represent the attractive (such as HB), van der Waals (vdW), and repulsive (such as steric) interactions, respectively. It should be mentioned that the isosurface value is 0.5. The left, middle, and right regions from -0.05 to 0.05 for sign ($\lambda_2\rho$) also represent the attractive, vdW, and repulsive interactions in Fig S8(b). The Fig S8 indicates that there are both the strong HB interaction and strong $\pi-\pi$ stacking interactions in amorphous pentamer, which probably influences on the spectroscopic properties of the amorphous uracil.

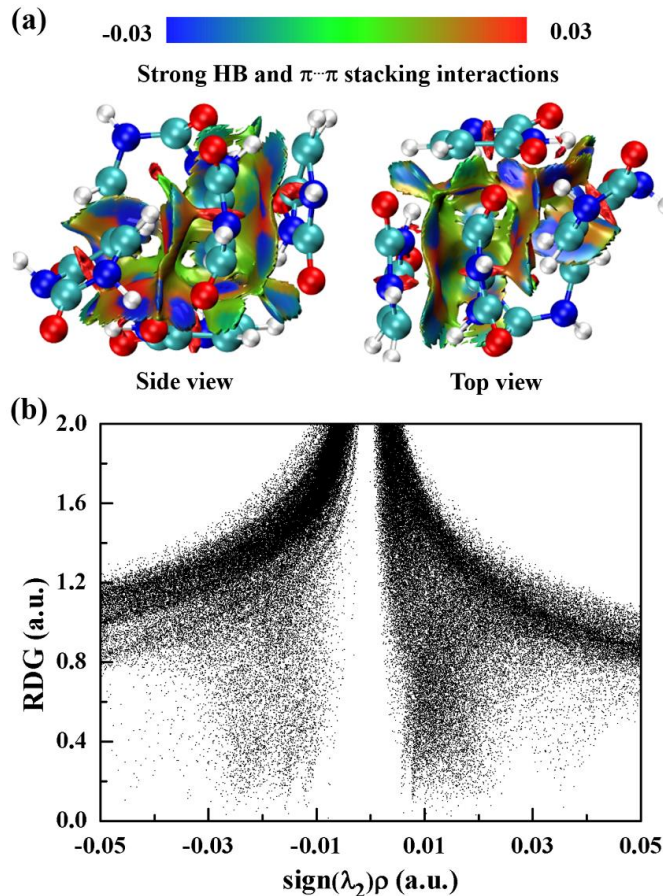


Fig S8. The reduced density gradient as a function of the electron density multiplied by the sign of the second Hessian eigenvalue. The data analyses for (a) gradient isosurfaces and (b) gradient values on cuboid grids of an amorphous pentamer cluster.

10. T-aggregation packing for amorphous uracil molecules

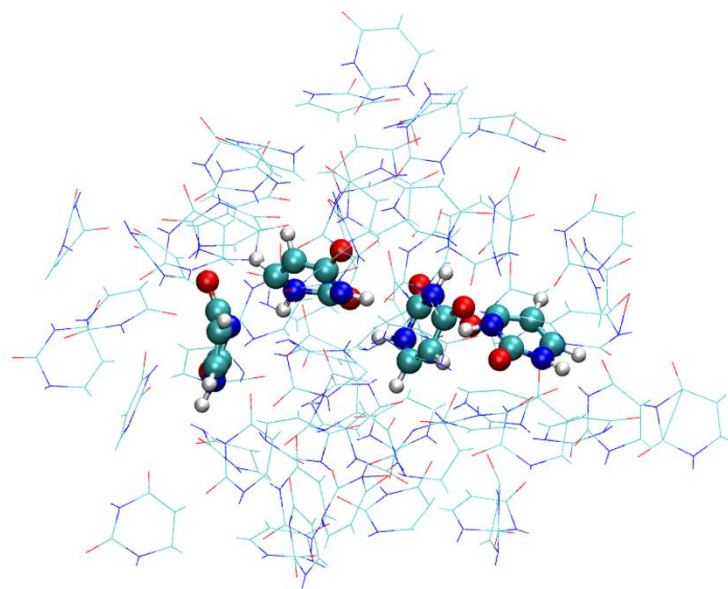


Fig S9. The schematic diagram of T-aggregation packing for amorphous uracil molecules.

11. Binding energies of all trimers in crystal

System					
E _{int}	-13.62	-1.05	-14.63	-3.30	-1.50
Symbol					
Trimer 1		$E_{\text{int}} = -31.44 \approx \textcircled{1} + \triangle{3} + \star{4} = -31.55$			
Trimer 2		$E_{\text{int}} = -14.85 \approx \textcircled{1} + \textsquare{2} = -14.67$			
Trimer 3		$E_{\text{int}} = -31.80 \approx \textcircled{1} + \triangle{3} + \star{4} = -31.55$			
Trimer 4		$E_{\text{int}} = -17.21 \approx \triangle{3} + \star{4} = -17.93$			
Trimer 5		$E_{\text{int}} = -4.77 \approx \textsquare{2} + \star{4} = -4.35$			
Trimer 6		$E_{\text{int}} = -5.92 \approx \textsquare{2} + \star{4} + \textsquare{5} = -5.85$			
Trimer 7		$E_{\text{int}} = -6.04 \approx \textsquare{2} + \star{4} + \textsquare{5} = -5.85$			
Trimer 8		$E_{\text{int}} = -6.05 \approx \textsquare{2} + \star{4} + \textsquare{5} = -5.85$			
Trimer 9		$E_{\text{int}} = -18.01 \approx \textcircled{1} + \textsquare{2} + \textsquare{5} = -16.17$			

Fig S10. The schematic diagram of binding energies E_{int} (in kcal/mol) for trimers from crystal of uracil, which can be almost combined with the binding energies of five dimers as a basic building block.

12. Binding energies of all tetramers in crystal

System					
	E _{int}				
Symbol	1	2	3	4	5
Tetramer 1		$E_{\text{int}} = -48.65 \approx 1 + 3 + 3 + 4 + 4 = -49.48$			
Tetramer 2		$E_{\text{int}} = -32.97 \approx 1 + 1 + 2 + 2 + 5 + 5 = -32.34$			
Tetramer 3		$E_{\text{int}} = -11.98 \approx 4 + 4 + 5 + 5 = -9.6$			
Tetramer 4		$E_{\text{int}} = -13.24 \approx 4 + 4 + 4 + 5 + 5 = -12.9$			
Tetramer 5		$E_{\text{int}} = -34.86 \approx 3 + 3 + 5 + 5 + 5 = -33.76$			
Tetramer 6		$E_{\text{int}} = -30.16 \approx 3 + 3 + 5 = -30.76$			
Tetramer 7		$E_{\text{int}} = -32.97 \approx 1 + 1 + 2 + 2 + 5 + 5 = -32.34$			
Tetramer 8		$E_{\text{int}} = -10.08 \approx 2 + 2 + 4 + 4 + 5 = -10.20$			
Tetramer 9		$E_{\text{int}} = -9.72 \approx 2 + 2 + 4 + 4 + 5 = -10.20$			
Tetramer 10		$E_{\text{int}} = -34.92 \approx 2 + 2 + 3 + 3 + 5 + 5 = -32.34$			
Tetramer 11		$E_{\text{int}} = -34.56 \approx 2 + 2 + 3 + 3 + 5 + 5 = -32.34$			
Tetramer 12		$E_{\text{int}} = -21.10 \approx 2 + 3 + 4 + 5 = -20.48$			
Tetramer 13		$E_{\text{int}} = -36.53 \approx 1 + 2 + 3 + 5 + 5 + 5 = -33.80$			
Tetramer 14		$E_{\text{int}} = -20.71 \approx 2 + 3 + 4 + 5 = -20.48$			

Fig S11. The schematic diagram of binding energies E_{int} (in kcal/mol) for tetramers from crystal of uracil, which can be almost combined with the binding energies of five dimers as a basic building block.

13. The RDG analysis of a tetramer cluster in crystal

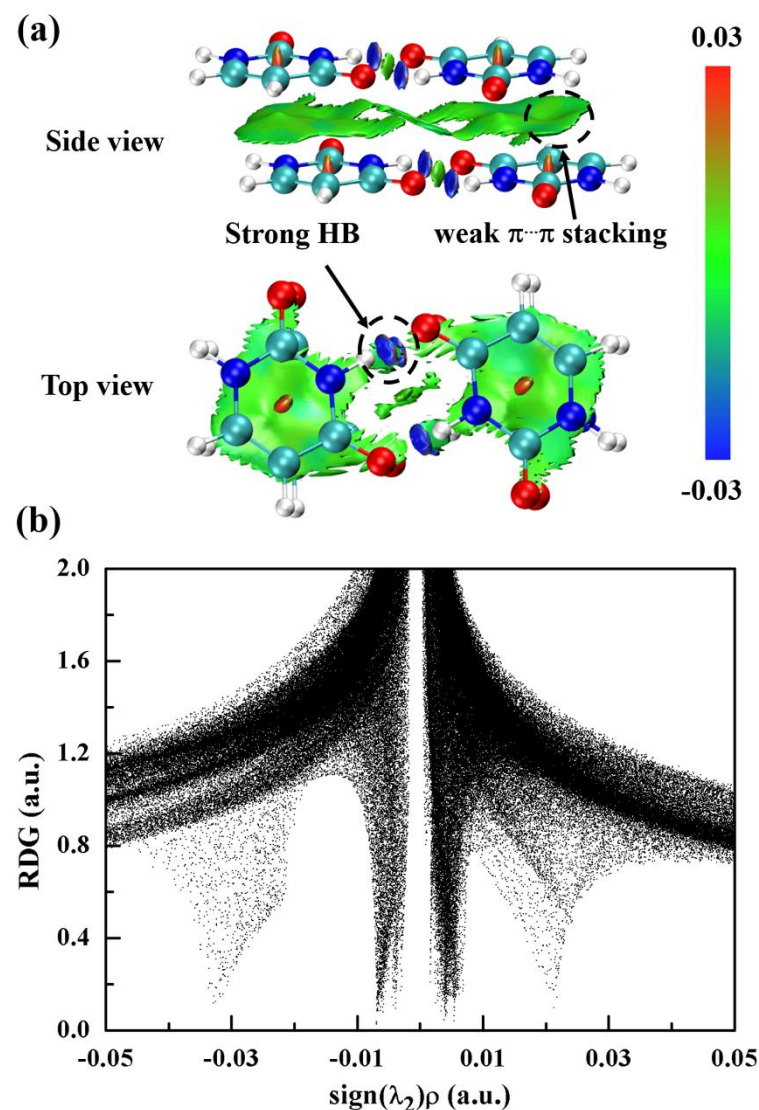


Fig S12. The reduced density gradient as a function of the electron density multiplied by the sign of the second Hessian eigenvalue. The data analyses for (a) gradient isosurfaces and (b) gradient values on cuboid grids of a tetramer cluster in the crystal of uracil.

14. The absorption spectra with virous TDDFT functionals in crystal

Table S2. The maximum absorption wavelengths (λ , nm) and the corresponding oscillator strength (f) for monomer, dimer, and trimer models calculated at TDDFT level using the ω B97X-D, M06-2X, CAM-B3LYP functionals with the 6-311++G(d, p) basic set (models with 10 Å background charges).

System	ω B97X-D		M06-2X		CAM-B3LYP	
	λ	f	λ	f	λ	f
monomer	227.1	0.06	230.0	0.01	227.0	0.10
dimer 1	230.8	0.16	230.1	0.16	231.4	0.16
dimer 2	236.5	0.01	236.2	0.01	237.2	0.01
trimer 1	232.3	0.36	231.4	0.33	232.8	0.36
trimer 2	237.1	0.01	237.1	0.02	237.8	0.01
tetramer 1	234.0	0.45	233.2	0.43	234.6	0.45
tetramer 2	230.7	0.19	238.36	0.01	231.1	0.19

15. Frontier molecular orbitals of dimer and trimer clusters in crystal

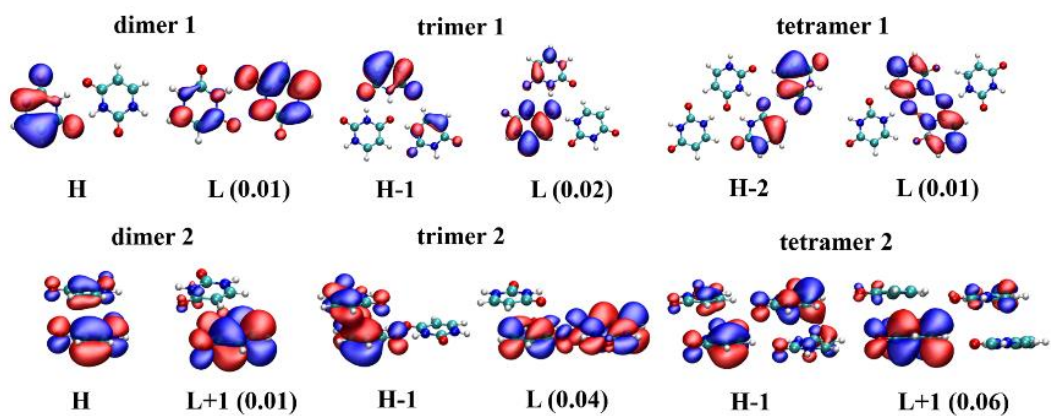


Fig S13. Frontier molecular orbitals (H: HOMO; L: LUMO) involved in the $\pi - \pi^*$ transition of dimer, trimer, and tetramer models, and the corresponding values of charge transfer are shown in parentheses. The calculations are employed at the TD-B3LYP/6-311++G(d, p) level.

16. The electrostatic potentials with charges of uracil in three condensed phases

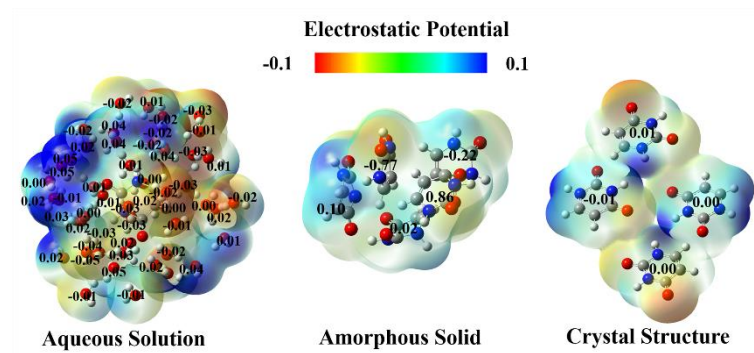


Fig S14. The electrostatic potentials with each monomer charge of uracil in aqueous solution, amorphous solid, and crystal.

17. The PBC-GEBF optimized Cartesian coordinates of uracil crystal.

Note: The initial structure (CIF ID: 1278441) is obtained from Ref 2.

C	1.7737239900	2.5787437300	-0.0094060500
C	2.0660192000	0.1410100000	0.0584542800
C	3.4757501400	0.3373689500	0.1980277700
C	3.9536372300	1.6036072800	0.2183258200
H	5.0110098100	1.8342882600	0.3051790400
H	3.5385795200	3.6337670700	0.0862044700
H	0.2865045400	1.1771229900	-0.0978236300
H	4.1262121600	-0.5253117800	0.2714271800
N	3.1331082800	2.6880294900	0.1089494500
N	1.3060163100	1.2859803200	-0.0339929300
O	1.0198353700	3.5376439600	-0.0843062500
O	1.4835560600	-0.9589022900	0.0116702400
C	2.3003191100	8.7600195600	3.0322073900
C	8.2704828900	9.7872346400	3.0337964300
C	7.7364693900	3.5987382900	-0.0096069100
C	2.0070855100	6.3221238400	2.9680089100
C	7.9779416300	12.2226595600	2.9654949100
C	8.0290961400	6.0361332200	0.0565444000
C	0.5916299200	6.5227482300	2.8256295000
C	6.5634865200	12.0194561100	2.8236563400
C	9.4411703300	5.8368407900	0.1945952100
C	0.1171487000	7.7858876900	2.8048823800
C	6.0873438600	10.7556767300	2.8043762500
C	9.9171802500	4.5725078100	0.2157458800
H	-0.9362906800	8.0248623200	2.7167526200
H	5.0333277800	10.5187254900	2.7108994800
H	10.9706259300	4.3315375900	0.2937199600
H	0.5365847400	9.8173973300	2.9364042800
H	6.5079964900	8.7255415000	2.9267567400
H	9.4857069000	2.5359695300	0.0695877400
H	3.7940639500	7.3725439300	3.1226603400
H	9.7675527600	11.1787703300	3.1113947600
H	6.2460714500	4.9857886800	-0.1113738000
H	-0.0589202100	5.6624544300	2.7507684500
H	5.9124834500	12.8785990100	2.7444947700

H	10.0847154600	6.7023403000	0.2577097400
N	0.9387888600	8.8692720800	2.9167612100
N	6.9066043300	9.6745332300	2.9252508100
N	9.0922168600	3.4885292900	0.1181521800
N	2.7702351800	7.4654186000	3.0616140000
N	8.7408723100	11.0828871400	3.0636285800
N	7.2667223100	4.8905640900	-0.0301639700
O	3.0516801400	9.7164385300	3.1072973700
O	9.0149175800	8.8291888000	3.1173619300
O	6.9815907500	2.6384107800	-0.0758122900
O	2.5641154400	5.2148475900	3.0149793300
O	8.5328548700	13.3334168500	3.0231413300
O	7.4641333700	7.1418088600	0.0274311900
tv	11.89467521	0.03253184	-0.03209595
tv	0.01875870	12.33602266	0.00698357
tv	-1.86241638	0.00689633	3.04449138

18. Reference:

1. G. S. Parry, *Acta Cryst.*, 1954, **7**, 313–320.
2. R. F. Stewart and L. H. Jensen, *Acta Cryst.*, 1967, **23**, 1102–1105.
3. E. R. Johnson, S. Keinan, P. Mori-Sanchez, J. Contreras-García, A. J. Cohen and W. Yang, *J. Am. Chem. Soc.*, 2010, **132**, 6498–6506.
4. A. J. Cohen, P. Mori-Sánchez and W. Yang, *Science*, 2008, **321**, 792–794.
5. T. Lu and F. Chen, *J. Comput. Chem.* 2012, **33**, 580–592.